ADVANCED MATERIALS

DOI: 10.1002/adma.2007001839

Liquid Crystalline Peptide Nanowires**

By *Tae Hee Han*, *Jangbae Kim*, *Ji Sun Park*, *Chan Beum Park*, *Hyotcherl Ihee*,* and *Sang Ouk Kim**

Nature frequently utilizes molecular self-assembly in generating functional nanostructures.[1–4] Unlike synthetic self-assembly usually driven by undirectional weak forces, the assembly of biomolecules is dominated by highly specific interactions such as hydrogen bonding or π-π stacking,[5,6] thereby readily producing hierarchical architecture that accommodates complex functionalities. A variety of nanostructured materials possessing diverse chemical or biological functionalities have been synthesized utilizing highly specific intermolecular interactions among nucleic acids,[7] proteins and peptides,[2–4,8–12] etc. However, the research effort to organize those nanostructured materials in a large scale is still in infancy.[13–15]

One dimensional nanomaterials have gathered particular attentions as building blocks for various nanoscale devices.[16,17] They provides a variety of attractive properties including anisotropic mechanical and electrical properties, low percolation threshold, etc.[17,18] Furthermore, when these anisotropic nanomaterials are individually dispersed, they spontaneously organize into liquid crystalline ordering. Diverse synthetic or natural nanomaterials ranging from semiconductor nanorods[19] or carbon nanotubes[20,21] to the tobacco mosaic virus[22,23] exhibit a variety of liquid crystalline ordering. Since liquid crystalline materials possess liquid-like fluidity as well as crystal-like ordering, their alignment is tunable by an external field. Frederiks transition, where the large scale orientation of liquid crystalline materials is manipulated by an external field, has long been utilized in commercial optical devices.[24]

We report the synthesis and liquid crystalline behaviors of novel peptide nanowires. The liquid crystalline nanowires were simply assembled from an aromatic dipeptides consisting of two successively connected phenylalanine units, well known as a structural motif for Alzheimer plaque.[10] The chemical structure of the dipeptide is shown in Figure 1a. Pre-

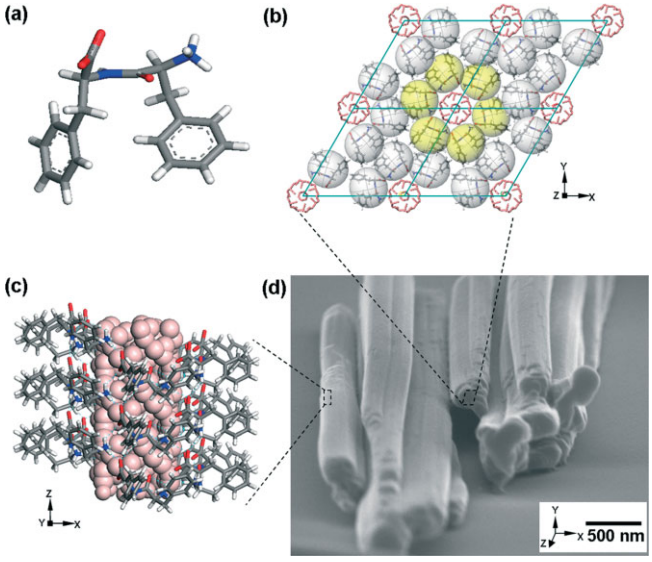

Figure 1. Schematic representation showing molecular arrangement of dipeptide in a peptide nanowire synthesized in nonpolar CS_2 solvent. a) Molecular conformation of the dipeptide molecule. Grey and white color represents carbon and hydrogen atoms respectively while red and blue color represents hetero atoms of oxygen and nitrogen. b) Hexagonal array of dipeptide molecules around central water molecules. Each dipeptide molecule was expressed with ball type geometry and six balls of yellow color show hexagonal array around water molecules of light purple. The structure was obtained from Pawley and Rietveld refinements by using a known crystal structure [25]. All dipeptide molecules are restrained in their position by two types of intermolecular hydrogen bonding (FF - FF and FF-water) and the outer diameter of an individual nanotube was around 2.4 nm. Each nanowire which is a bundle of helical nanotubes was formed by the hydrophobic nature of phenyl rings in dipeptide molecules. c) 3D model of the self-assembly of dipeptide into helical architecture by multilayer hydrogen bonding. The self-assembly of the dipeptide molecules occurs in a right-handed helical fashion. Each turn of a helix contains six dipeptide molecules. (d) SEM image of the nanowires. SEM analysis reveals that the average diameter of the nanowires was (346 ± 103.9) nm, the length (8.6 ± 4.4) nm, and the aspect ratio (25.1 ± 11.1).

[*] Prof. S. O. Kim, T. H. Han, J. S. Park, Prof. C. B. Park
Department of Materials Science and Engineering, KAIST Institute for the Nanocentury
Korea Advanced Institute of Science and Technology (KAIST)
Daejeon 305-701 (Korea)
E-mail: sangouk.kim@kaist.ac.kr
Prof. H. Ihee, J. Kim
National Creative Research Initiative Center for Time-Resolved Diffraction Department of Chemistry and School of Molecular Science (BK21)
KAIST Institute for the Nanocentury
Korea Advanced Institute of Science and Technology (KAIST)
Daejeon 305-701 (Korea)
E-mail: hyotcherl.ihee@kaist.ac.kr

[**] We thank Dr C. M. Koo and Prof. D. G. Churchill for helpful discussions, and M. J. Woo for assisting with the powder diffractometer system. This work was supported by the Korea Research Foundation (KRF-2005-003-D00085), Creative Research Initiatives (Center for Time-Resolved Diffraction) of MOST/KOSEF, the second stage of the Brain Korea 21 Project, the Basic Research Program of the Korea Science &Engineering Foundation (R01-2005-000-10456-0), and the Korean Ministry of Science and Technology, the Fundamental R&D Program for Core Technology of Materials funded by the Ministry of Commerce, Industry and Energy, Korea. Supporting Information is available online from Wiley InterScience or from the author.

vious studies by Gazit et al. revealed that the dipeptides assemble into robust nanotubes in an aqueous medium and can be applied as a useful template for casting metallic nanowires.[10,26–29] We discovered that it forms individually-dispersed rigid nanowires in an organic solvent. Due to the rigidity and high aspect ratio of the nanowires, they formed colloidal liquid crystalline phase for a broad concentration range. The liquid crystallinity in a highly volatile organic solvent was particularly advantageous for the rapid fabrication of well-aligned morphology over a broad area.

The synthetic procedure for liquid crystalline peptide nanowires is remarkably simple. Predetermined amounts of dipeptide and carbon disulfide (CS_2) were sealed in a vial. Sonication of the vial at ambient temperature led to rigid nanowires, individually dispersed in CS_2. Figure 1d shows a scanning electron micrograph of the synthesized nanowires. Note that the nanowires individually dispersed in CS_2 aggregated upon drying. Despite a simple preparation process and rapid assembly, they had fairly narrow size distribution revealing a low polydispersity index of 1.25 (Supporting Information, Fig. S1). The average diameter and length of nanowires were 346 nm and 8.6 μm, respectively, providing a high aspect ratio of 25.1. The nanowires consisting of aromatic peptides were highly rigid such that their persistence lengths were identical to their entire lengths.

The unit cell and molecular arrangement determined by analyzing powder diffraction pattern with Pawley and Rietveld refinement (Supporting Information, Fig. S2) show hexagonal arrangement in the cross section (Fig. 1b) and helical packing structure in a side view (Fig. 1c). In the cross section of a nanowire, aqueous columns are hexagonally packed, and enclosed by the hydrophilic portion of peptides. Note that the water molecules in the aqueous column were initially included in the as-received peptide material in the form of the powered crystal. The lateral packing of peptides around the aqueous column follows a right-handed helical direction. The length of a single pitch was 5.46 Å, consisting of six dipeptides. The assembly of peptides in nonpolar CS_2 imposed the minimization of interfacial area between assembled structure and surrounding solvent, resulting in nanowire morphology. This has less surface area than the nanotube morphology, previously observed by Gazit et al., which has additional surface exposed to the surrounding aqueous medium at the inner side of the tube structure. Despite the difference in their nanoscale morphologies, however, the molecular arrangement in nanowires obtained from the refining process was nearly identical to that of a single crystal or nanotubes.[25,30]

The peptide nanowires could be individually dispersed in CS_2 up to a high concentration of over 10 wt % without any aggregation or precipitation. This high stability of dispersion is largely owing to the low density of nanowires (1.299 g cm^{-3} from molecular modeling) comparable to that of CS_2 (1.263 g cm^{-3}). The dispersions including more than 0.2 wt % of nanowires showed the optical birefringence of the liquid crystalline phase as soon as the dispersion was prepared. The photographs for a series of dispersions placed between two crossed polarizers are presented in Figure 2a. To investigate the equilibrium phase behavior, the dispersion was kept stationary until the phase separation was completed. The dispersion including 0.5–7 wt % of nanowires spontaneously phase-separated into isotropic and birefringent phases, indicating an isotropic to liquid crystalline phase transition. Such a broad phase transition range originated from the polydispersity of nanowires.[31,32] The sedimented anisotropic phase showed morphology that dark and bright brushes were interwoven, signifying a nematic liquid crystalline phase. Isolation and drying of each separated phase revealed that the

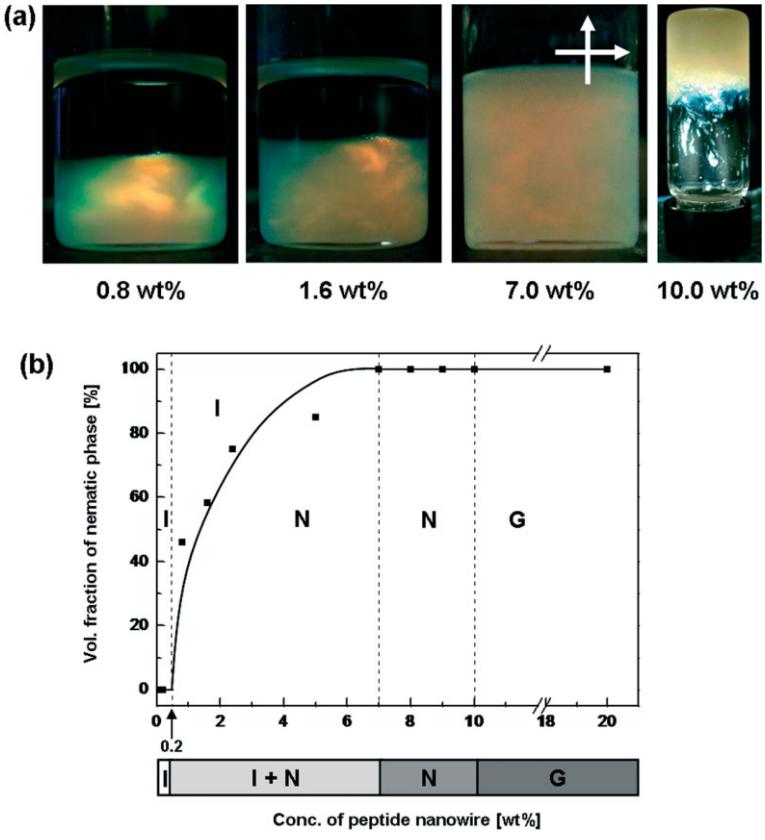

Figure 2. Photographs of liquid crystalline peptide nanowire dispersions between crossed polarizers and phase diagram for nanowire dispersion as a function of nanowire concentration. a) Glass vials of nanowire dispersions between crossed polarizers. Samples were stationary for more than six months to complete phase separation. Isotropic phase (dark) is distinguished from the birefringent nematic liquid crystalline phase (yellow). b) Phase diagram showing the volume fraction [%] of the nematic phase as a function of nanowire concentration [wt %]. The peptide nanowire dispersion underwent phase transitions; I (isotropic phase) – I + N (biphasic state) – N (nematic phase) – nematic gel or nematic glass. The biphase ranged from 0.2 wt % to 7 wt %. In the biphasic range, the volume fraction of the nematic phase increased with the concentration of nanowire. At a high concentration over 10 wt %, nematic gel or nematic glass appeared.

ADVANCED MATERIALS

nanowires in the isotropic phase were shorter than those in nematic phase. The average lengths of nanowires in the isotropic and nematic phases were 5.0 and 9.7 μm, respectively (Supporting Information, Fig. S3). Upon shaking these dispersions, the anisotropic phase spread out rapidly throughout the sample. The optical birefringence was enhanced by shear-induced alignment of nanowires (Supporting Information, Fig. S4). For a concentration from 7 to 10 wt %, the entire dispersion showed optical birefringence without any phase separation. Above the high concentration of 10 wt %, birefringent dispersion showed mechanical elasticity, a typical behavior of nematic gel or nematic glass. On the basis of experimental findings, the phase diagram for peptide nanowire dispersion is established in Figure 2b. The phase transitions through isotropic phase – biphase (coexistence of isotropic and nematic phases) – nematic phase – nematic gel or nematic glass phase were summarized as a function of nanowire concentration. Note that no distinct thermal phase transition behavior was observed below 46 °C, the boiling temperature of CS_2.

Figure 3a shows optical micrographs of liquid crystalline nanowire dispersion located between a pair of crossed polarizers. A drop of dispersion was sealed between two slide glasses and characterized upon a polarized light microscopy. The Schlieren texture, a characteristic morphology of nematic liquid crystalline phase, was observed. The yellow arrow indicates the junction point of two emanating white brushes. Upon rotating the polarizers, these brushes rotated in the same direction with an angular velocity twice as fast as that of polarizers. This observation indicates +1/2 disclination of nematic liquid crystals. After complete evaporation of solvent, the arrangement of nanowires was observed by a scanning electron microscopy, as shown in Figure 3b. Due to their rigidity, the arrangement of nanowires was significantly disfigured upon drying. However, typical director orientation around a pair of positive and negative half disclinations was distinct as indicated.

The liquid-like fluidity of nematic dispersion allowed for the control over the macroscopic alignment of nanowires by applying an electric field. A droplet of dispersion was deposited between two oppositely charged electrodes located upon a slide glass. As presented in Figure 4, rapid evaporation of solvent left well-aligned nanowires oriented along the direction of electric field. In regions b and c, the nanowires were aligned following the arcs of electric field. In region d where electric field is uniformly applied between two electrodes, the nanowires were well-aligned in a uniform density over a broad area. The cooperative alignment of nanowires in nematic ordering yielded well-aligned morphology in a rapid process.

In summary, liquid crystalline peptide nanowires have been demonstrated as novel materials for nanofabrication. The nanowires individually dispersed in an organic solvent could be readily assembled from an aromatic dipeptide. The stable dispersion of nanowires exhibited colloidal liquid crystalline phase for a broad concentration range, allowing the rapid alignment of nanowires under an external field. Simply depositing a drop of liquid crystalline nanowire dispersion and immediate drying under an electric field yielded a well-aligned morphology of nanowires over a broad area. Our work presents that the hierarchical organization of liquid crystalline peptide nanowires consisting of highly specific peptide assembly and nanoscale liquid crystalline ordering provides an efficient pathway to a novel nanoarchitecture. The potential application of liquid crystalline peptide nanowires includes nanopatterning, reinforcing materials for nanocomposites, etc.[8,13–15]

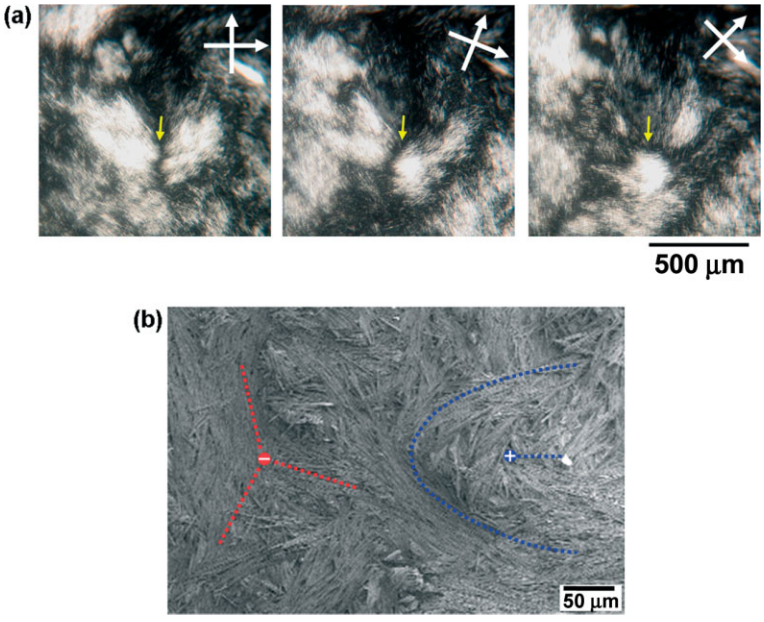

Figure 3. A series of polarized optical micrographs of liquid crystalline peptide nanowire dispersions. (a) Effects of a clockwise rotation of the crossed polarizers. A series of optical micrographs was taken from successive rotations of crossed polarizers. Rotating degrees were 0°, 22.5° and 45°. Micrographs show a Schileren texture of nematic liquid crystalline phase. The yellow arrow indicates the junction point of two emanating white brushes. Two brushes rotate at the angular velocity twice as fast as those of crossed polarizers in the same direction. Scale bar: 500 μm. (b) SEM image of peptide nanowires in a dried sample. The arrangement of nanowires around a pair of half disclinations (±1/2) was observed. Blue and red lines indicate +1/2 and –1/2 strength disclinations, respectively.

Experimental

The lyophilized form of the NH_2-Phe-Phe-COOH dipeptide was purchased from Bachem (Bubendorf, Switzerland). CS_2 was purchased from Merck (Germany) and used as-received. To prepare peptide nanowire dispersion, a predetermined amount of dipeptide (0.05–20 wt %) was dissolved in CS_2 and sealed in a glass vial. Sonicating for 20 min at ambient temperature simply led to individually dispersed peptide nanowires. The optical birefringence of the prepared dispersion was characterized by observing the sample sealed in a vial or between a pair of slide glasses located between crossed polarizers. To investigate the equilibrium phase behavior of dispersions in biphasic region, the samples preserved stationary more than six months were characterized. The phase separation of isotropic and nematic phases was mostly completed in two months revealing the exact volume fraction

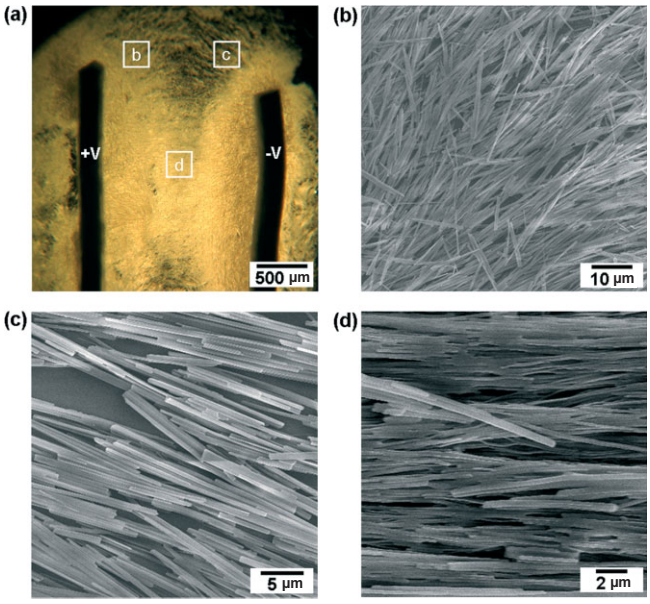

Figure 4. Electric field induced alignment of liquid crystalline peptide nanowires. a) Optical microscope image of electrically aligned nanowires. The applied electric field strength was 125 mV μm^{-1} (distance: 1600 µm, voltage: 200 V). A droplet of liquid crystalline nanowire dispersion (1 wt %) was deposited between two electrodes and air-dried; SEM images for nanowire alignment as indicated in (a). Close-up of an each point, near the anode (b), near the cathode (c) and half way (d) between electrodes, indicates well aligned nanowires.

of each phase. The samples for powder X-ray diffraction were prepared by evaporating CS_2 of a dispersion and subsequent grinding of the residue. The X-ray diffraction measurements were performed on a Rigaku D maxIIIc powder diffractometer with CuKa radiation (λ = 1.5418 Å). A sample for scanning electron microscope was prepared by drying a drop of dispersion upon a slide glass. Carbon coating was performed to enhance scattering contrast and electric conductivity (CED 030 carbon evaporator, Bal-tec, Germany). The prepared sample was analyzed upon a field emission scanning electron microscopy (FEI Sirion, Netherlands).

Structural Analysis and Modeling: The obtained experimental powder diffraction pattern in the range 2–50° (2θ) was very similar with simulated powder diffraction pattern of the previously reported single crystal structure taken from Cambridge Crystallographic Data Center (CCDC No. 163340) [25]. With this unit cell structure, we performed Pawley refinement to search detailed unit cell information in which pseudo-Voigt function was applied to fit whole peak profiles and Berar-Baldinozzi function was selected for asymmetry correction. After several iteration steps, the R_{WP} value of 5.16 % was obtained. In addition, to elucidate detailed information of molecular arrangement in obtained unit cell, Rietveld refinement procedure was performed and the results are shown in Figure S2. The translational movements of dipeptide were expressed by introducing motion groups (grey balls) and all torsional angles were chosen as fitting parameters in optimizing the lattice and pattern parameters. Finally, March–Dollase function was selected to consider preferred orientation effect and global isotropic temperature factor was introduced in structure solution as well. The final R_{WP} value after iterative Rietveld refinement was 9.37 %. The optimized cell parameters and information are as follows: Hexagonal, $P6_1$, a = 24.1610 Å, b = 24.1610 Å, c = 5.4515 Å, α = 90.0°, β = 90.0°, γ = 120.0°, Z = 6, V = 2755.97 $Å^3$. To investigate the influence of water molecules upon the crystal structure we performed overall refinement process without any water molecules. The R_{WP} value of the final Rietveld refinement was above 50 %, from which we could conclude that water molecules are indispensible for the crystal structure. Most of the molecular modeling, Pawley and Rietveld refinement were carried out using *Reflex* [33], a software package for crystal structure determination from powder diffraction pattern, implemented in MS modeling v4.1 (Accelrys Inc.).

Received: July 27, 2007
Revised: August 29, 2007

[1] M. Sarikaya, C. Tamerler, A. K. Y. Jen, K. Schulten, F. Baneyx, *Nat. Mater.* **2003**, *2*, 577.
[2] S. Zhang, *Nat. Biotechnol.* **2003**, *21*, 1171.
[3] J. D. Hartgerink, E. Beniash, S. I. Stupp, *Science* **2001**, *294*, 1684.
[4] D. T. Bong, T. D. Clark, T. R. Granja, M. R. Ghadiri, *Angew. Chem. Int. Ed.* **2001**, *40*, 988.
[5] G. M. Whitesides, J. P. Mathias, C. T. Seto, *Science* **1991**, *254*, 1312.
[6] G. C. L. Wong, J. X. Tang, A. Lin, Y. Li, P. A. Janmey, C. R. Safinya, *Science* **2000**, *288*, 2035.
[7] P. W. K. Rothemund, *Nature* **2006**, *440*, 297.
[8] X. Gao, H. Matsui, *Adv. Mater.* **2005**, *17*, 2037.
[9] A. Aggeli, L. A. Nyrkova, R. Harding, L. Carrick, T. C. B. McLeish, A. N. Semenov, N. Boden, *Proc. Natl. Acad. Sci. USA* **2001**, *98*, 11857.
[10] M. Reches, E. Gazit, *Science* **2003**, *300*, 625.
[11] A. M. Corrigan, C. Müller, M. R. H. Krebs, *J. Am. Chem. Soc.* **2006**, *128*, 14740.
[12] V. Percec, A. E. Dulcey, V. S. K. Balagurusamy, Y. Miura, J. Smidrkal, M. Peterca, S. Nummelin, U. Edlund, S. D. Hudson, P. A. Heiney, D. A. Hu, S. N. Magonov, S. A. Vinogradov, *Nature* **2004**, *430*, 764.
[13] M. Reches, E. Gazit, *Nat. Nanotechnol.* **2006**, *1*, 195.
[14] A. M. Hung, S. I. Stupp, *Nano Lett.* **2007**, *7*, 1165.
[15] P. Mesquida, D. L. Ammann, C. E. MacPhee, R. A. McKendry, *Adv. Mater.* **2005**, *17*. 893.
[16] Y. Huang, X. Duan, Q. Wei, C. M. Lieber, *Science* **2001**, *291*, 630.
[17] Y. Xia, P. Yang, Y. Sun, Y. Wu, B. Mayers, B. Gates, Y. Yin, F. Kim, H. Yan, *Adv. Mater.* **2003**, *15*, 353.
[18] X. Duan, Y. Huang, R. Agarwal, C. M. Lieber, *Nature* **2003**, *421*, 241.
[19] L. S. Li, L. Manna, A. P. Alivisatos, *Nano Lett.* **2002**, *2*, 557.
[20] W. Song, I. A. Kinloch, A. H. Windle, *Science* **2003**, *302*, 1363.
[21] L. M. Ericson, H. Fan, H. Q. Peng, V. A. Davis, W. Zhou, J. Sulpizio, Y. H. Wang, R. Booker, J. Vavro, C. Guthy, A. N. G. Parra-Vasquez, M. J. Kim, S. Ramesh, R. K. Saini, C. Kittrell, G. Lavin, H. Schmidt, W. W. Adams, W. E. Billups, M. Pasquali, W. F. Hwang, R. H. Hauge, J. E. Fischer, R. E. Smalley, *Science* **2004**, *305*, 1447.
[22] C. Mao, D. J. Solis, B. D. Reiss, S. T. Kottmann, R. Y. Sweeney, A. Hayhurst, G. Georgiou, B. Iverson, A. M. Belcher, *Science* **2004**, *303*, 213.
[23] S. W. Lee, C. Mao, C. E. Flynn, A. M. Belcher, *Science* **2002**, *296*, 892.
[24] P. G. de Gennes, J. Prost, in *The Physics of Liquid Crystals*, Clarendon, Oxford **1993**.
[25] C. H. Görbitz, *Chem. Eur. J.* **2001**, *7*, 5153.
[26] N. Kol, L. Adler-Abramovich, D. Barlam, R. Z. Shneck, E. Gazit, I. Rousso, *Nano Lett.* **2005**, *5*, 1343
[27] S. L. Sedman, L. Adler-Abramovich, S. Allen, E. Gazit, S. J. B. J. Tendler, *J. Am. Chem. Soc.* **2006**, *128*, 6903.
[28] O. Carny, D. E. Shalev, E. Gazit, *Nano Lett.* **2006**, *6*, 1594.
[29] N. Hendler, N. Sidelman, M. Reches, E. Gazit, Y. Rosenberg, S. Richter, *Adv. Mater.* **2007**, *19*, 1485.
[30] C. H. Görbitz, *Chem. Commun.* **2006**, 2332.
[31] M. A. Bates, D. Frenkel, *J. Chem. Phys.* **1999**, *110*, 6553.
[32] A. Stroobants, H. N. W. Lekkerkerker, T. Odijk, *Macromolecules* **1986**, *19*, 2232.
[33] Accelrys, *Material Studio Release Notes, Release 4.1*, Accelrys Software, San Diego **2006**.

